Hindawi
Journal of Nanomaterials
Volume 2019, Article ID 1592621, 8 pages
https://doi.org/10.1155/2019/1592621

Research Article

Double Plasmon Resonance Nanostructured Silver Coatings with Tunable Properties

Anna Kuzminova,[1] Pavel Solař,[1] Peter Kúš,[2] and Ondřej Kylián[1]

[1]*Department of Macromolecular Physics, Faculty of Mathematics and Physics, Charles University, Prague 8, Prague 180 00, Czech Republic*
[2]*Department of Surface and Plasma Science, Faculty of Mathematics and Physics, Charles University, Prague 8, Prague 180 00, Czech Republic*

Correspondence should be addressed to Ondřej Kylián; ondrej.kylian@gmail.com

Received 30 November 2018; Accepted 25 February 2019; Published 1 April 2019

Academic Editor: Lucien Saviot

Plasmonic materials that exhibit dual or multiple localised surface plasmon resonances (LSPRs) due to their high application potential in biosensing and biodetection are gaining increasing attention. Here, we report on the novel strategy suitable for the production of silver nanostructured dual-LSPR coatings. This fully vacuum-based technique uses a magnetron sputtering of Ag and a gas aggregation source of silver nanoparticles. It is shown that when combined, produced Ag nano-islands and nanoparticles exhibit due to their different sizes and shapes two independent LSPRs in the visible part of spectra. Furthermore, the intensities and positions of individual LSPR may be precisely controlled by the amount of sputter-deposited nano-islands and a number of Ag nanoparticles, which opens new possibilities for the tailor-made production of novel platforms for surface-enhanced spectroscopic biodetection.

1. Introduction

Recent rapid advances in the fabrication of various types of nanoparticles and nanomaterials with well-defined properties open new and fascinating opportunities in terms of the production of materials with advanced functionalities. A typical example in which the nanofabrication plays the role of enabling technology is the production of platforms suitable for highly sensitive spectroscopic biodetection and biosensing techniques, such as surface-enhanced Raman spectroscopy (SERS) or surface-enhanced fluorescence (SEF) [1–12]. These techniques benefit from the ability of metallic nanoparticles to strongly enhance the local electromagnetic field that, in turn, reinforces the interaction of the incident light with molecules in the vicinity of metal particles. The electromagnetic field (EMF) enhancement, which may be attributed to the excitation of LSPR, based on the collective oscillation of a cloud of free electrons within the metal nanoparticle, reaches its maximum value when the frequency of incoming light matches the LSPR [8]. The position and the intensity of the LSPR peaks are strongly linked with the material from which the nanoparticles are formed, as well as with their shape (e.g., [13, 14]).

Thus, all of these properties have to be controlled to achieve the highest EMF enhancement needed for optimal SERS or SEF activity of the fabricated nanomaterials. This may be achieved by numerous techniques that employ both top-down and bottom-up preparation strategies, including sputtering or cluster beam deposition [15–17]. In addition, today, considerable attention is given to materials that exhibit multiple LSPR peaks, as they may trigger the development of multifunctional platforms that will combine more detection techniques on a single platform or will enable to use multiple light sources operated at different wavelengths and to multiplex them [18, 19]. Moreover, as already shown theoretically [20] and experimentally [21], the dual-LSPR materials offer strong field enhancements, both in the excitation and scattering wavelengths, which, in turn, may lead to the significant total enhancement of the detected SERS signal. From this point of view, the possibility to produce surfaces with dual-

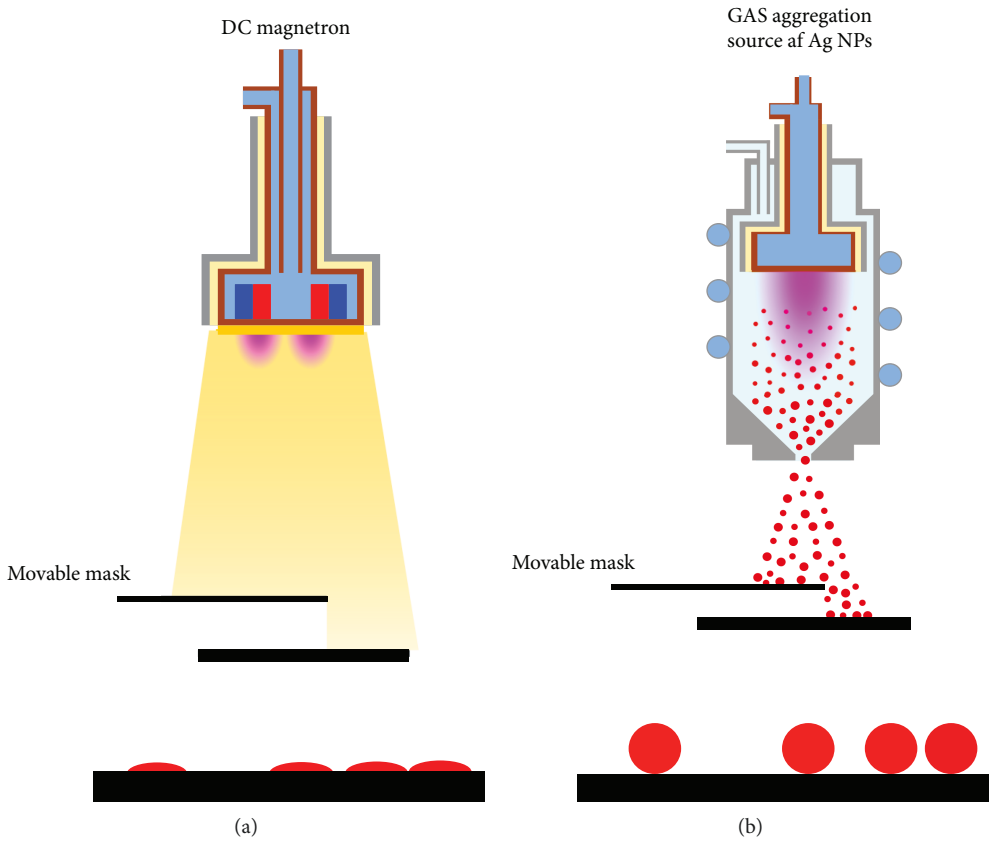

Figure 1: Schematic pictures of (a) magnetron sputtering of silver and (b) GAS of Ag NPs.

LSPR at desired wavelengths is crucial for the assurance of the enhanced performance of SERS active substrates.

Two general strategies are proposed for the fabrication of dual- or multi-LSPR metallic materials. The first group is based on the combination of two or more materials that are arranged in different nano-architectures (e.g., mixtures of NPs from two metals [22, 23], core-shell nanoparticles [24–29], or sandwiched structures in which individual metallic NPs are separated by a dielectric layer [23, 30]). However, the necessity to use two or more materials makes the fabrication process rather complex and often laborious. This limitation may be overcame by the second family of strategies that uses single material nanostructures with special shapes (e.g., nano-rods with various aspect ratios, nano-stars, and bowties [21, 31–35]) or by a combination of single material nanostructures with different sizes and shapes (e.g., a mixture of flat triangular/hexagonal and smaller close-to-spherical nanoparticles [36]).

The prevailing methods employed for the production of single material multipeak LSPR surfaces are chemical synthesis and lithography, which provide precise control of the properties of the formed nano-objects. However, these methods also pose certain disadvantages that relate, for example, to the need to use potentially harmful solvents, or precursors, whose handling and disposal require high safety precautions, or low throughput of nanolithography, which makes these techniques unsuitable for large-scale production.

The main goal of this study is to demonstrate that silver dual-peak LSPR coatings may be effectively produced by a simple vacuum-based technique that combines sputter deposition of silver nano-islands with the deposition of Ag nanoparticles (NPs) by means of a gas aggregation source. Furthermore, to show that this strategy makes it possible to vary both the separation of individual LSPR peaks and their intensities, a novel approach based on the production of coatings with gradient plasmonic properties is adopted.

2. Materials and Methods

Silver nano-islands were deposited by means of water-cooled, planar DC magnetron, equipped with a silver target (81 cm in diameter, 3 mm thick, declared purity 99.99%). The magnetic circuit with an intensity of 0.2 mT above the erosion track enabled to operate the magnetron at low pressure (0.07 Pa), which is needed for the directionality of the flux of the sputtered silver. The magnetron was operated in a constant current mode with a current of 100 mA. This value corresponded to the voltage on the magnetron of 365 V. The distance between the target and substrate holder was 100 mm.

Ag nanoparticles were produced by a Haberland-type gas aggregation source (GAS) [37]. This source is based on a DC planar magnetron (81 mm in diameter) introduced into a water-cooled aggregation chamber. The aggregation chamber (inner diameter: 102 mm) was terminated by a cone with an orifice of 1.5 mm. The distance between the target and the

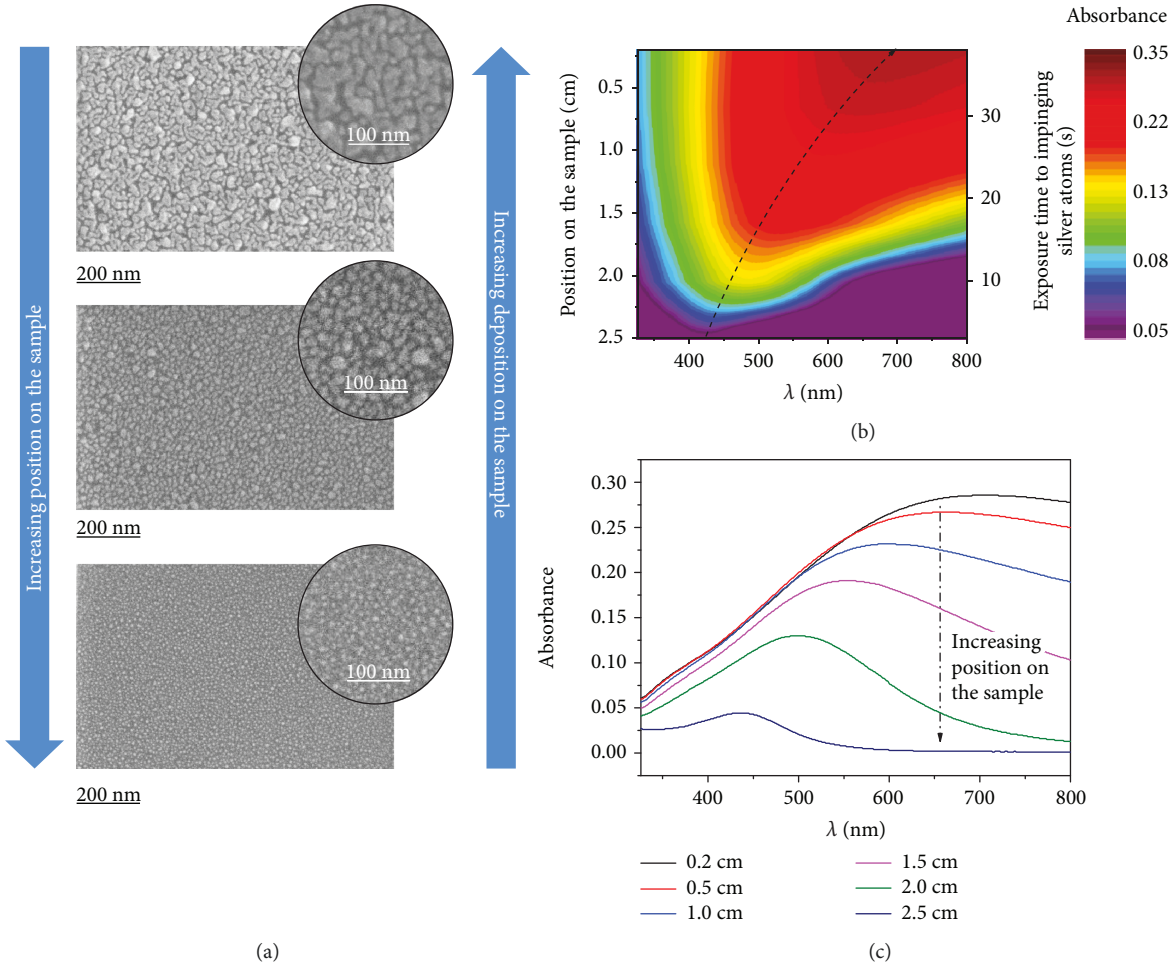

Figure 2: (a) SEM images of Ag nano-island films taken at different positions on the gradient sample. (b) Absorbance measured at different positions on the gradient sample. The dashed line corresponds to the wavelength at which the intensity of the LSPR peak is maximal. Clear redshift of the LSPR may be seen with decreasing position on the sample. (c) Examples of acquired UV-vis spectra of Ag nano-island films at different positions on the gradient sample. The speed of the movable mask was 4 cm/min.

output orifice was approximately 150 mm. GAS was installed onto a main vacuum deposition chamber. The deposition was performed at a pressure of 50 Pa in the aggregation chamber (Ar flow: 5 sccm), whereas the pressure in the main deposition chamber was below 0.01 Pa. The magnetron was powered by a DC power supply. The current used in this study was 200 mA, which resulted in the voltage on the magnetron of 291 V. The distance between the output orifice of the GAS and the substrate holder was 280 mm.

Both magnetron sputtering and GAS systems enabled to produce spatially homogeneous nano-island or nanoparticle arrays on a surface area, having at least 4 cm in diameter. In addition to spatially homogeneous deposition, both deposition setups were designed to enable the preparation of 1D gradients. To achieve this, a movable mask was introduced above the substrate to be coated (distance between the mask and the substrate was 1 mm), as schematically shown in Figure 1. The mask initially shielded the entire surface of the substrate. Simultaneously, with the start of the deposition of Ag nanostructures (either nano-islands or nanoparticles), the shield began to move with a constant speed in the direction along the sample length (i.e., the area of the substrate reachable by the incoming Ag species or Ag NPs gradually increased with time). As a result, various locations on the substrate experienced different silver or silver NP deposition times, which resulted in the formation of 1D gradient coatings. The position on the sample that corresponds to the initial position of the mask (i.e., the position exposed for the longest time to incoming species/NPs) is denoted as 0 cm in the subsequent text.

As substrates were used either one-side polished Si wafers (ON Semiconductor, Czech Republic) or soda lime glass slides (Marienfeld) pre-coated with a C : F film. Fluorocarbon film (30 nm thick) was deposited by the RF magnetron sputtering of a polytetrafluoroethylene target in an argon atmosphere (for details, see [38]). The morphology of produced samples was determined by scanning electron microscopy (SEM) using a Mira3 microscope (TESCAN). SEM images were acquired at different magnifications in a secondary electron mode with the energy of the electron beam at 30 keV. Optical properties of silver nanostructured coatings were measured by UV-vis spectrophotometry. A Hitachi 2910 spectrophotometer was used, and the absorption spectra were recorded in the range from 325 nm to 800 nm.

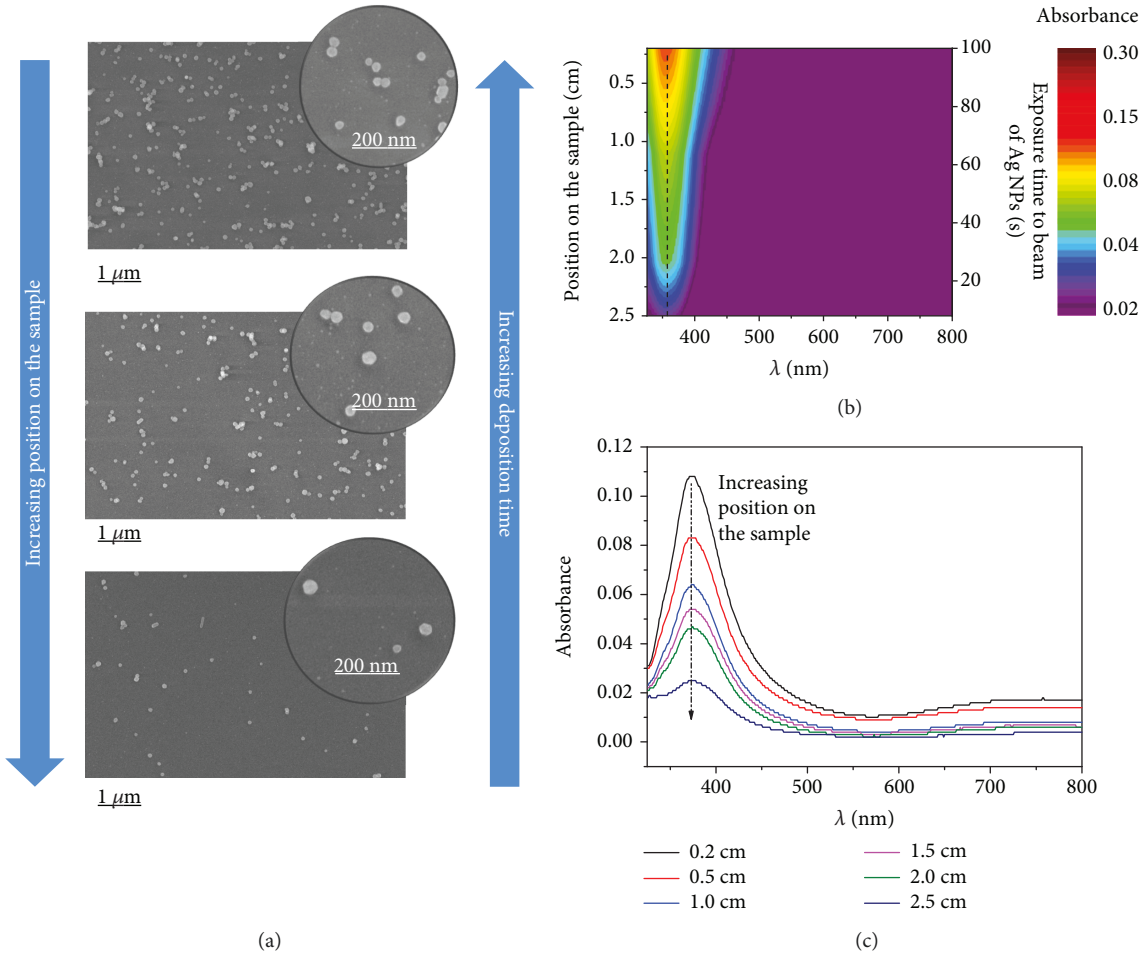

Figure 3: (a) SEM images of Ag nanoparticle gradient films deposited by GAS taken at different positions on the sample. (b) Absorbance measured at different positions on the samples. The dashed line corresponds to the wavelength at which the LSPR peak was observed. No variation of LSPR position was observed along the sample length. (c) Examples of acquired UV-vis spectra of Ag nanoparticle films. The speed of the movable mask was 1.5 cm/min.

3. Results and Discussion

To highlight the advantages arising from the combination of silver magnetron sputtering with the deposition of Ag NPs by means of GAS, the first step of this study was to separately characterise the coatings prepared by these two techniques. In agreement with previous studies [39–42], the magnetron sputtering results in the formation of Ag nano-islands whose size and separation depend on the time by which the substrate is exposed to the flux of incoming silver atoms emitted from the sputtered target. As seen in Figure 2(a), the position on the sample that corresponds to a low fluence of silver is characterised by a large number of well-separated small Ag nano-islands. The increase of the deposition time, which is, in this case, realised by the movable mask (speed: 4 cm/min), subsequently, leads to the gradual growth of the size of formed nanostructures and to the decrease of the mean gap between them.

This is consistent with the growth model that assumes (1) surface diffusion of Ag atoms, (2) formation of stable dimmers when two diffusing atoms meet, (3) growth of the nano-islands by capturing new incoming atoms, and (4) coalescence of growing nano-islands (e.g., [43]). Such changes in the morphology of the growing silver films in the direction parallel to the direction of the movement of the mask cause progressive changes in the plasmonic properties along the sample length. This is demonstrated in Figures 2(b) and 2(c): the redshift of the position of LSPR peak and increase of its intensity was observed with the decreasing position on the samples (i.e., with increasing deposition time). This closely corresponds to previous studies that reported variations of the LSPR peak position depending on the size [44] and mutual distance between individual metallic nanostructures [45, 46].

Completely different behaviour may be observed when the GAS of silver NPs is used. In contrast to sputter deposition, Ag NPs are formed, in this case, already in the aggregation chamber of the GAS. As a result, the increasing deposition time has no impact on the size and shape of the deposited Ag NPs and leads solely to the increase in their number on the substrate. This effect, also observed in other metallic NPs produced by the GAS system (e.g., copper [47]), may be seen in Figure 3(a); whereas Ag nanoparticles have a spherical shape with a mean diameter of 55 ± 12 nm

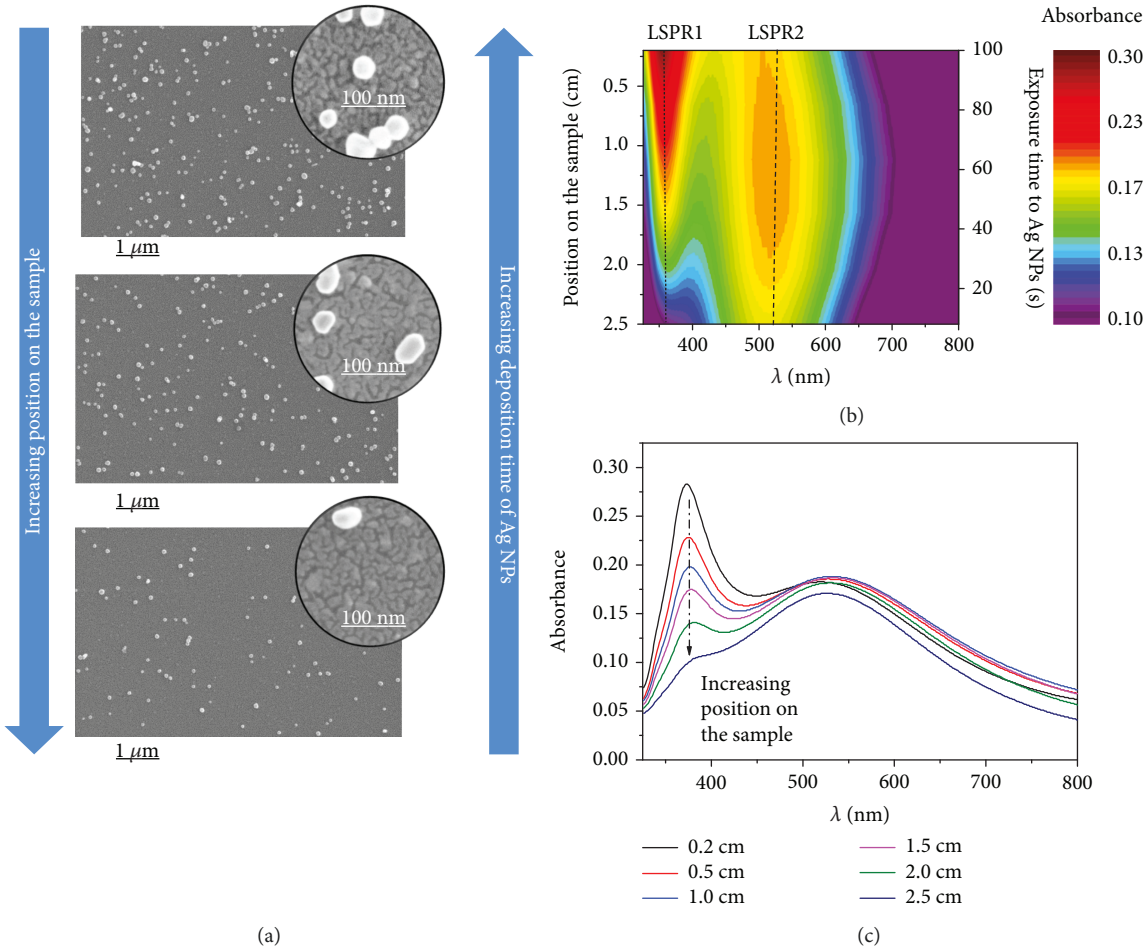

Figure 4: (a) SEM images of gradient Ag nanoparticle films deposited by GAS (speed of the movable mask: 1.5 cm/min) on the substrate preseeded with Ag nano-islands (deposition time: 20 s) taken at different positions on the sample. (b) Absorbance measured at different positions on the samples. Two well-separated peaks may be seen. LSPR1 corresponds to Ag NPs, while LSPR2 is due to the Ag nano-island films. As highlighted by dashed lines, no variations in the positions of both LSPR peaks were observed along the sample length. (c) Examples of UV-vis spectra acquired on the gradient film.

independent of the position on the sample, the number of deposited Ag NPs linearly decreases in the direction of the movement of the mask (i.e., with decreasing exposure time of the substrate to the beam of incoming Ag NPs). The same size of Ag NPs and the high mean distances between individual Ag NPs, which avoid the shift in the LSPR position due to the dipole-dipole interaction between them [45], in turn, assure constant positioning of the LSPR peak. Thus, increasing the exposure time leads only to the increase of LSPR intensity (see Figure 3(b)).

In the next step, both deposition techniques were combined. Two different situations were investigated. In the first one, the entire substrate was first homogeneously preseeded with sputter deposited Ag nano-island films (deposition time: 20 s) that were subsequently decorated by the gradient film of Ag NPs (speed of the movable mask: 1.5 cm/min). As the nano-island and nanoparticle depositions are two independent processes, the morphology of the resulting coatings is a simple combination of both. This is demonstrated in Figure 4(a), where SEM images acquired on various positions on the gradient sample are presented. Whereas the base layer of the Ag nano-island film has on all positions on the sample approximately of the same morphology, the amount of Ag NPs deposited by GAS decreases with the decreasing time of substrate exposure to the beam of incoming Ag NPs. In addition, due to the significantly different sizes of the Ag nano-islands and Ag NPs, the plasmonic properties of the resulting coatings were also found to be a superposition of the plasmonic properties of the sputter deposited Ag films and arrays of Ag NPs. Because of this, two distinct LSPR peaks were detected—the first belongs to Ag NPs (denoted as LSPR1) and the second corresponds to the nano-islands (denoted as LSPR2) (see Figure 4(b)). As the deposition time of the Ag nano-islands was the same for all positions on the sample (20 s), the spectral position and the intensity of the LSPR2 peak remained the same along the sample length. Furthermore, in analogy to GAS-based deposition, as shown in Figure 3, the position of the LSPR1 peak does not depend on the Ag NPs deposition time, and thus, only its intensity changes and follows the gradient of the Ag NP surface density. In other words, the results presented in Figure 4 show that by a combination of Ag sputter deposition and GAS

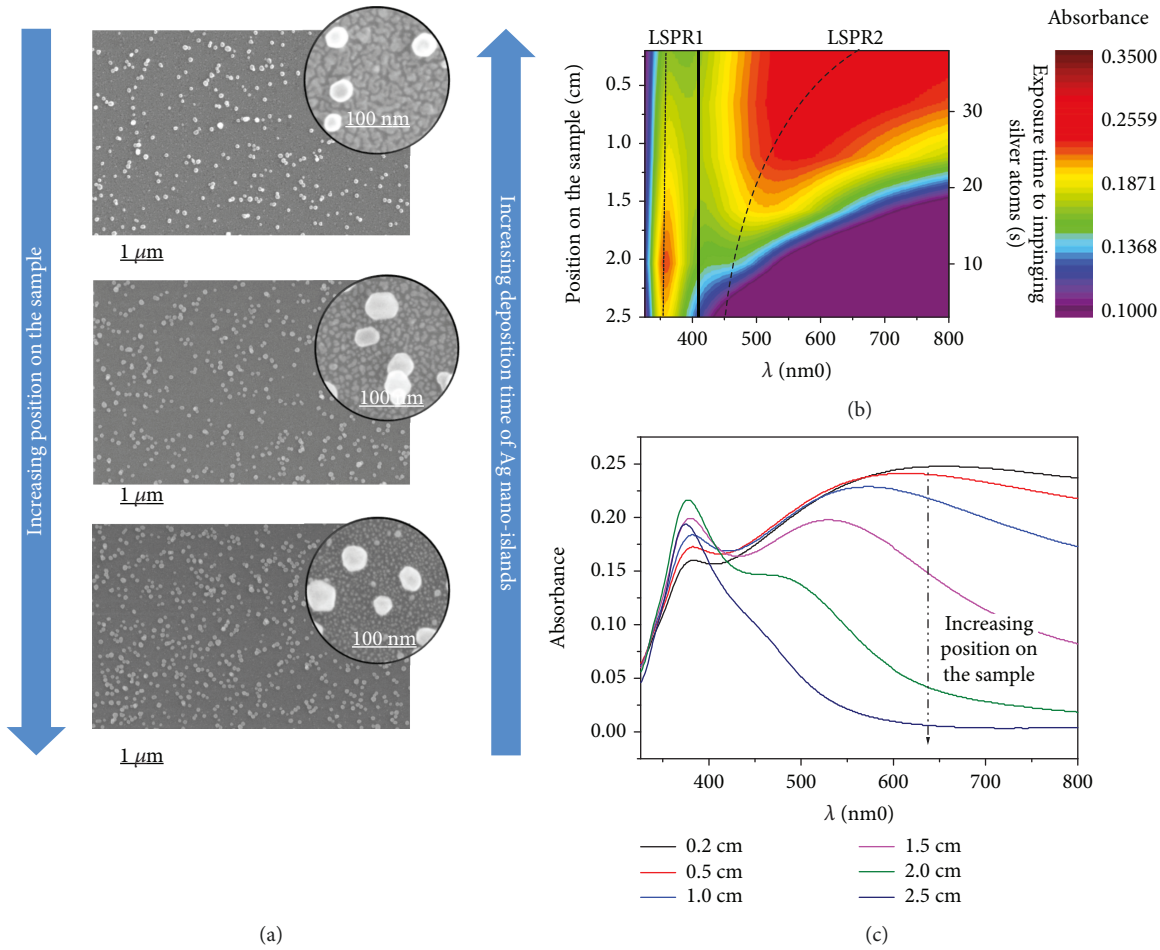

Figure 5: (a) SEM images of Ag nanoparticle films deposited by GAS (deposition time: 1 min) on substrate preseeded with the gradient film of Ag nano-islands taken at different positions on the sample (speed of the movable mask: 4 cm/min). (b) Absorbance measured at different positions on the samples. Two well-separated peaks may be seen. LSPR1 corresponds to Ag NPs, while LSPR2 is due to the Ag nano-island films. As highlighted by dashed lines, while no change of the position of the LSPR1 peak was observed along the sample length, significant redshift in the position of the LSPR2 peak with the deposition time of Ag nano-islands is evident. (c) Examples of acquired UV-vis spectra of Ag nanoparticle films.

deposition, it is possible to prepare single material dual-LSPR peak coatings with adjustable ratios between intensities of individual LSPR peaks.

Finally, to check the possibility of also tailoring the distance between two LSPR peaks, substrates were coated by the gradient film of Ag nano-islands (speed of the movable mask: 4 cm/min) and, subsequently, decorated by the fixed and spatially homogeneous amount of Ag NPs (deposition time: 1 min). Again, the morphology and the plasmonic properties of the resulting coatings may be described as a simple combination of properties of nano-islands and nanoparticles, and two independent LSPR peaks were observed. Moreover, as is demonstrated in Figure 5, the plasmonic peak that corresponds to the Ag nano-islands (LSPR2) shifts to higher wavelengths and increases its intensity from the side of the gradient sample, which was exposed shortly by the impinging Ag atoms to the side that was in sight of view of the sputtered silver for a longer time. In contrast, the peak that corresponds to the Ag NPs deposited by means of GAS maintains its position at about 370 nm. However, due to the overlap of both LSPR peaks, the absorbance measured at the maximum of LPSR1 peak changed along the sample length.

4. Conclusions

This study has introduced a novel, simple, and fully vacuum-based strategy suitable for the production of single material dual-LSPR peak coatings that combines sputter deposition of Ag nano-islands with the deposition of Ag NPs by means of a GAS aggregation source. It shows that this technique not only enables the production of dual-LSPR coatings but also makes it possible to tailor both the spectral separation of individual LSPR peaks and the ratio of their intensity. This is a very important result, mainly with respect to the possible use of such produced plasmonic substrates as platforms for biodetection and biorecognition. Furthermore, due to the vacuum character of the fabrication procedure, no solvents or precursors are required, which then avoids the necessity of thoroughly cleaning the produced materials from the residues, which is often necessary when chemical synthesis is employed. This, together with the short deposition times

and the possibility to coat relatively large surface areas (square centimetres), makes this technique a highly interesting alternative to the techniques commonly employed for the production of multipeak LSPR materials.

Data Availability

The datasets used to support the findings of this study are available from the corresponding author upon request.

Conflicts of Interest

The authors declare that there is no conflict of interest regarding the publication of this paper.

Acknowledgments

This work was supported by the Grant Agency of the Czech Republic (GACR 18-10897S). A.K. also acknowledges support from the Charles University Research Centre Program (UNCE/SCI/010). The authors are grateful to Professor H. Biederman for fruitful discussions.

References

[1] D. L. Jeanmaire and R. P. Van Duyne, "Surface Raman spectroelectrochemistry," *Journal of Electroanalytical Chemistry and Interfacial Electrochemistry*, vol. 84, no. 1, pp. 1–20, 1977.

[2] M. G. Albrecht and J. A. Creighton, "Anomalously intense Raman spectra of pyridine at a silver electrode," *Journal of the American Chemical Society*, vol. 99, no. 15, pp. 5215–5217, 1977.

[3] K. Sokolov, G. Chumanov, and T. M. Cotton, "Enhancement of molecular fluorescence near the surface of colloidal metal films," *Analytical Chemistry*, vol. 70, no. 18, pp. 3898–3905, 1998.

[4] A. M. Glass, P. F. Liao, J. G. Bergman, and D. H. Olson, "Interaction of metal particles with adsorbed dye molecules: absorption and luminescence," *Optics Letters*, vol. 5, no. 9, p. 368, 1980.

[5] K. Kneipp, H. Kneipp, I. Itzkan, R. R. Dasari, and M. S. Feld, "Ultrasensitive chemical analysis by Raman spectroscopy," *Chemical Reviews*, vol. 99, no. 10, pp. 2957–2976, 1999.

[6] R. A. Alvarez-Puebla and L. M. Liz-Marzán, "SERS-based diagnosis and biodetection," *Small*, vol. 6, no. 5, pp. 604–610, 2010.

[7] B. Sharma, R. R. Frontiera, A.-I. Henry, E. Ringe, and R. P. Van Duyne, "SERS: materials, applications, and the future," *Materials Today*, vol. 15, no. 1-2, pp. 16–25, 2012.

[8] S. Schlücker, "Surface-enhanced Raman spectroscopy: concepts and chemical applications," *Angewandte Chemie*, vol. 53, no. 19, pp. 4756–4795, 2014.

[9] M. Jahn, S. Patze, I. J. Hidi et al., "Plasmonic nanostructures for surface enhanced spectroscopic methods," *Analyst*, vol. 141, no. 3, pp. 756–793, 2016.

[10] C. Zong, M. Xu, L. J. Xu et al., "Surface-enhanced Raman spectroscopy for bioanalysis: reliability and challenges," *Chemical Reviews*, vol. 118, no. 10, pp. 4946–4980, 2018.

[11] H. Tang, C. Zhu, G. Meng, and N. Wu, "Review—surface-enhanced Raman scattering sensors for food safety and environmental monitoring," *Journal of the Electrochemical Society*, vol. 165, no. 8, pp. B3098–B3118, 2018.

[12] I. Bruzas, W. Lum, Z. Gorunmez, and L. Sagle, "Advances in surface-enhanced Raman spectroscopy (SERS) substrates for lipid and protein characterization: sensing and beyond," *Analyst*, vol. 143, no. 17, pp. 3990–4008, 2018.

[13] M. Rycenga, C. M. Cobley, J. Zeng et al., "Controlling the synthesis and assembly of silver nanostructures for plasmonic applications," *Chemical Reviews*, vol. 111, no. 6, pp. 3669–3712, 2011.

[14] J. J. Mock, M. Barbic, D. R. Smith, D. A. Schultz, and S. Schultz, "Shape effects in plasmon resonance of individual colloidal silver nanoparticles," *The Journal of Chemical Physics*, vol. 116, no. 15, pp. 6755–6759, 2002.

[15] G. Santoro, S. Yu, M. Schwartzkopf et al., "Silver substrates for surface enhanced Raman scattering: correlation between nanostructure and Raman scattering enhancement," *Applied Physics Letters*, vol. 104, no. 24, article 243107, 2014.

[16] P. Žvátora, P. Řezanka, V. Prokopec, J. Siegel, V. Švorčík, and V. Král, "Polytetrafluorethylene-Au as a substrate for surface-enhanced Raman spectroscopy," *Nanoscale Research Letters*, vol. 6, no. 1, p. 366, 2011.

[17] O. Polonskyi, P. Solař, O. Kylián et al., "Nanocomposite metal/plasma polymer films prepared by means of gas aggregation cluster source," *Thin Solid Films*, vol. 520, no. 12, pp. 4155–4162, 2012.

[18] Y. Wang and L. Tang, "Multiplexed gold nanorod array biochip for multi-sample analysis," *Biosensors & Bioelectronics*, vol. 67, no. 24, pp. 18–24, 2015.

[19] J. Zhu, J. Li, and J. Zhao, "Obtain quadruple intense plasmonic resonances from multilayered gold nanoshells by silver coating: application in multiplex sensing," *Plasmonics*, vol. 8, no. 3, pp. 1493–1499, 2013.

[20] J. Ye and P. VanDorpe, "Nanocrosses with highly tunable double resonances for near-infrared surface-enhanced Raman scattering," *International Journal of Optics*, vol. 2012, Article ID 745982, 5 pages, 2012.

[21] J. Lin, Y. Zhang, J. Qian, and S. He, "A nano-plasmonic chip for simultaneous sensing with dual-resonance surface-enhanced Raman scattering and localized surface plasmon resonance," *Laser Photonics Reviews*, vol. 8, no. 4, pp. 610–616, 2014.

[22] H. Ishii, Y. Ishikawa, D. Nagao, and M. Konno, "Unary- or binary-plasmonic nanoparticle-assemblies formed within hollow silica particles with a surfactant-assisted method," *Materials Letters*, vol. 221, pp. 256–259, 2018.

[23] M. Petr, O. Kylián, A. Kuzminova et al., "Noble metal nanostructures for double plasmon resonance with tunable properties," *Optical Materials*, vol. 64, pp. 276–281, 2017.

[24] P. Mulvaney, M. Giersig, and A. Henglein, "Electrochemistry of multilayer colloids: preparation and absorption spectrum of gold-coated silver particles," *The Journal of Physical Chemistry*, vol. 97, no. 27, pp. 7061–7064, 1993.

[25] Q. Li and Z. Zhang, "Broadband tunable and double dipole surface plasmon resonance by TiO_2 core/Ag shell nanoparticles," *Plasmonics*, vol. 6, no. 4, pp. 779–784, 2011.

[26] Y. Li, B.-P. Zhang, C.-H. Zhao, L. Zou, and J.-X. Zhao, "Synthesis and optical absorption properties of Au–Ag nanoparticle bimetal dispersed SiO_2 composite films," *Journal of Materials Research*, vol. 29, no. 02, pp. 221–229, 2014.

[27] F. Shirzaditabar, M. Saliminasab, and B. Arghavani Nia, "Triple plasmon resonance of bimetal nanoshell," *Physics of Plasmas*, vol. 21, no. 7, article 072102, 2014.

[28] A. Steinbrück, A. Csáki, G. Festag, and W. Fritzsche, "Preparation and optical characterization of core–shell bimetal nanoparticles," *Plasmonics*, vol. 1, no. 1, pp. 79–85, 2006.

[29] A. Vahl, J. Strobel, W. Reichstein et al., "Single target sputter deposition of alloy nanoparticles with adjustable composition via a gas aggregation cluster source," *Nanotechnology*, vol. 28, no. 17, article 175703, 2017.

[30] V. S. K. Chakravadhanula, M. Elbahri, U. Schürmann et al., "Equal intensity double plasmon resonance of bimetallic quasi-nanocomposites based on sandwich geometry," *Nanotechnology*, vol. 19, no. 22, article 225302, 2008.

[31] H.-H. Chang and C. J. Murphy, "Mini gold nanorods with tunable plasmonic peaks beyond 1000 nm," *Chemistry of Materials*, vol. 30, no. 4, pp. 1427–1435, 2018.

[32] J. Langer, S. M. Novikov, and L. M. Liz-Marzán, "Sensing using plasmonic nanostructures and nanoparticles," *Nanotechnology*, vol. 26, no. 32, p. 322001, 2015.

[33] C. L. Nehl, H. Liao, and J. H. Hafner, "Optical properties of star-shaped gold nanoparticles," *Nano Letters*, vol. 6, no. 4, pp. 683–688, 2006.

[34] E. Nalbant Esenturk and A. R. Hight Walker, "Surface-enhanced Raman scattering spectroscopy via gold nanostars," *Journal of Raman Specroscopy*, vol. 40, no. 1, pp. 86–91, 2009.

[35] C. R. Rekha, V. U. Nayar, and K. G. Gopchandran, "Synthesis of highly stable silver nanorods and their application as SERS substrates," *Journal of Science: Advanced Materials and Devices*, vol. 3, no. 2, pp. 196–205, 2018.

[36] N. Malikova, I. Pastoriza-Santos, M. Schierhorn, N. A. Kotov, and L. M. Liz-Marzán, "Layer-by-layer assembled mixed spherical and planar gold nanoparticles: control of interparticle interactions," *Langmuir*, vol. 18, no. 9, pp. 3694–3697, 2002.

[37] H. Haberland, M. Karrais, M. Mall, and Y. Thurner, "Thin films from energetic cluster impact: a feasibility study," *Journal of Vacuum Science & Technology A: Vacuum, Surfaces, and Films*, vol. 10, no. 5, pp. 3266–3271, 1992.

[38] M. Petr, O. Kylián, J. Hanuš et al., "Surfaces with roughness gradient and invariant surface chemistry produced by means of gas aggregation source and magnetron sputtering," *Plasma Processes and Polymers*, vol. 13, no. 6, pp. 663–671, 2016.

[39] C. Charton and M. Fahland, "Optical properties of thin Ag films deposited by magnetron sputtering," *Surface and Coatings Technology*, vol. 174-175, pp. 181–186, 2003.

[40] M. Schwartzkopf, A. Buffet, V. Körstgens et al., "From atoms to layers: in situ gold cluster growth kinetics during sputter deposition," *Nanoscale*, vol. 5, no. 11, pp. 5053–5062, 2013.

[41] M. Subr, M. Petr, O. Kylian, J. Kratochvil, and M. Prochazka, "Large-scale Ag nanoislands stabilized by a magnetron-sputtered polytetrafluoroethylene film as substrates for highly sensitive and reproducible surface-enhanced Raman scattering (SERS)," *Journal of Materials Chemistry C*, vol. 3, no. 43, pp. 11478–11485, 2015.

[42] J. Hanuš, H. Libenská, I. Khalakhan, A. Kuzminova, O. Kylián, and H. Biederman, "Localized surface plasmon resonance tuning via nanostructured gradient Ag surfaces," *Materials Letters*, vol. 192, pp. 119–122, 2017.

[43] P. Asanithi, S. Chaiyakun, and P. Limsuwan, "Growth of silver nanoparticles by DC magnetron sputtering," *Journal of Nanomaterials*, vol. 2012, 8 pages, 2012.

[44] K. L. Kelly, E. Coronado, L. L. Zhao, and G. C. Schatz, "The optical properties of metal nanoparticles: the influence of size, shape, and dielectric environment," *The Journal of Physical Chemistry B*, vol. 107, no. 3, pp. 668–677, 2003.

[45] P. K. Jain, W. Huang, and M. A. El-Sayed, "On the universal scaling behavior of the distance decay of plasmon coupling in metal nanoparticle pairs: a plasmon ruler equation," *Nano Letters*, vol. 7, no. 7, pp. 2080–2088, 2007.

[46] H. Yokota, T. Taniguchi, T. Watanabe, and D. Kim, "Control of localized surface plasmon resonance energy in monolayer structures of gold and silver nanoparticles," *Physical Chemistry Chemical Physics*, vol. 17, no. 40, pp. 27077–27081, 2015.

[47] O. Kylián, J. Kratochvíl, J. Hanuš, O. Polonskyi, P. Solař, and H. Biederman, "Fabrication of Cu nanoclusters and their use for production of Cu/plasma polymer nanocomposite thin films," *Thin Solid Films*, vol. 550, pp. 46–52, 2014.